

Effects of the isotopic composition on the fundamental gap of CuCl

A. Göbel, T. Ruf, M. Cardona, and C. T. Lin

Max-Planck Institut für Festkörperforschung, Heisenbergstrasse 1, D-70569 Stuttgart, Germany

J. Wrzesinski, M. Steube, and K. Reimann

Institut für Physik, Universität Dortmund, D-44221 Dortmund, Germany

J.-C. Merle and M. Joucla

Institut de Physique et Chimie des Matériaux, 23 rue du Loess, F-67037 Strasbourg, France

(Received 9 January 1998)

We have investigated the effects of isotopic composition on the band gap of CuCl on a series of samples made out of the stable isotopes ^{63}Cu , ^{65}Cu , ^{35}Cl , and ^{37}Cl . Besides specimens containing elements with the natural abundances, we have measured samples with monoisotopic sublattices as well as artificial mixtures of isotopes. With nonlinear (two-photon absorption, second-harmonic generation) and linear (luminescence) optical spectroscopy we find that the fundamental gap of CuCl *increases* by $364(18) \mu\text{eV}/\text{amu}$ when *increasing* the Cl mass. However, it *decreases* by $76(5) \mu\text{eV}/\text{amu}$ when *increasing* the Cu mass. Using a two-oscillator model for the lattice dynamics of CuCl we show that these rates are consistent with the anomalous increase of the band gap with increasing temperature. These effects can be traced back to the strong p - d mixing in the copper halides. From the temperature dependence of the band gap of CuBr we also estimate the changes of its gap with isotopic composition. [S0163-1829(98)06024-X]

I. INTRODUCTION

The influence of the isotopic composition of semiconductors on their physical properties has received considerable attention during the past decade. Results in the field have been reviewed in several publications.¹⁻⁴ Among the topics of recent interest are the influence of the isotopic composition on the lattice constant of germanium and of compound semiconductors^{5,6} or the changes in the thermal conductivity.⁷ In certain cases isotope substitution can be used either to discern the effects of isotope-disorder-induced phonon scattering from the anharmonic decay of phonons⁸ or to tune the efficiency of anharmonic decay channels.⁹ The energies and lifetimes of individual phonons in germanium as a function of isotope disorder were studied along several dispersion branches by means of inelastic neutron scattering.¹⁰ Changing the lattice-dynamical properties by means of isotope substitution also allows one to study the renormalization of the fundamental gap due to electron-phonon coupling and changes of the lattice constant.^{5,11-13}

Copper chloride is among the most ionic semiconductors that crystallize in the zinc-blende structure. Being close to phase transitions, it exhibits a number of peculiarities that have been associated with a strongly anharmonic lattice potential, e.g., a strongly negative linear expansion coefficient at low temperatures¹⁴ and elastic shear constants that decrease with increasing hydrostatic pressure.¹⁵ The anharmonic interaction of phonons in CuCl was also employed to explain the anomalous TO-phonon structure in its Raman spectrum as a Fermi resonance in which the optical phonon is pushed out of a two-phonon combination band.^{9,16,17} First-principles calculations on structural anomalies in the copper halides using all-electron density functional theory have predicted a large number of metastable off-center sites for Cu in

CuCl.^{18,19} Raman measurements on isotopically modified CuCl, however, showed that these off-center theories cannot explain the anomalous TO-phonon spectrum.⁹ Other first-principles calculations on the bulk properties and phonon frequencies do not reveal indications for off-center sites of Cu in CuCl.²⁰

Another unusual property of CuCl is the sizable increase of its fundamental gap with increasing temperature²¹⁻²³ and its inverted ($J = \frac{1}{2}, J = \frac{3}{2}$) valence band structure.²⁴ Many experimental results and calculations reveal that the admixture of copper d states to chlorine p states is crucial for the structure of the valence bands.

In this paper we deal with the renormalization of the CuCl band gap by the electron-phonon interaction. We use *isotope substitution* to selectively tune the phonon frequencies of the acoustic and optic modes in our samples and measure the changes in the band gap with nonlinear spectroscopy or luminescence at 2 K. In the case of chlorine substitution we find a gap *increase* when *increasing* the mass. This (usual) behavior has been observed so far in many elemental and compound semiconductors.⁵ In contrast, we find a *decreasing* band gap when *increasing* the copper mass. Changing the mass of one of the constituents changes the mean-square phonon amplitude and therefore *isotope substitution* effectively is analogous to *changing the temperature* of a compound. In general, the temperature dependence of the renormalization of the band gap results from a complicated interplay of (i) first- and second-order electron-phonon interactions that contribute to the energy of the conduction and valence bands, (ii) changes due to thermal lattice expansion, and (iii) changes in the phonon occupation number. In a simple model, we treat the band-gap renormalization as being caused by two harmonic oscillators, one at high (optic) and one at low (acoustic) phonon frequencies, which ap-

proximate the lattice dynamics of CuCl. This leads to simple expressions for the mass and temperature dependence of the band gap. Our analysis shows that the band gap of CuCl is already strongly renormalized by the zero-point motion of these acoustic- and optic-phonon oscillators. The former tends to increase the band gap while the latter decreases it.

The paper is organized as follows: In Sec. II we discuss the relevant properties of the CuCl band structure. Section III presents the experimental details, while the data are presented in Sec. IV. Section V briefly outlines the influence of the electron-phonon interaction on the gap renormalization by temperature and isotope mass and discusses the results in terms of a simple two-oscillator model. The conclusions are drawn in Sec. VI.

II. ELECTRONIC BAND STRUCTURE OF CuCl

In tetrahedrally coordinated compound semiconductors the upper valence bands and the lower conduction bands mainly stem from the s^2p^6 hybridization of the uppermost atomic states of the constituent atoms. Copper chloride is a prominent exception. The energies of the atomic copper d levels and of the atomic chlorine p levels are very similar. As a result, the copper d levels hybridize with the chlorine p levels and strongly affect the energies and the structure of the valence bands. A number of articles^{24–28} and reviews^{29,30} on the electronic band structure of CuCl exist in the literature. Therefore, we briefly summarize the details pertinent to our work only. For a more general and instructive discussion of the role of cation d states in II-VI compounds we refer to Ref. 31.

It was realized very early²⁴ that the spin-orbit splitting in CuCl is reversed as compared to all other direct gap zinc-blende semiconductors, i.e., the uppermost valence band is twofold degenerate having Γ_7 symmetry, while the next lower, fourfold degenerate valence band exhibits Γ_8 symmetry. This is due to the p - d mixing of the atomic orbitals and is illustrated in Fig. 1. The relevant atomic states of copper and chlorine are shown in column (a). When subjected to a crystal field of T_d symmetry, the orbital copper d levels split into two Γ_5 and one twofold degenerate Γ_3 levels. The former hybridize with the chlorine p levels having the same symmetry resulting in two threefold degenerate Γ_5 levels [Fig. 1(b)]. This hybridization raises the top of the valence band relative to the anion (Cl) p level, which in the absence of the cation d orbital would determine the valence band maximum. As a result, the band gap in the copper halides is much smaller than expected from the extrapolation of the band gaps in the series Ge, GaAs, ZnSe, and CuX ($X=\text{Cl,Br,I}$). Another indication for the important role of the Cu d levels is the fact that, although the p levels of the isoelectronic anions Cl, Br, and I differ by about 2 eV, the band gaps of the copper halides differ by less than 0.3 eV, i.e., the anion levels have only a small influence on the band gap.³¹ Taking the spin-orbit interaction into account results in a splitting of the p - d mixed Γ_5 states into levels of Γ_7 and Γ_8 symmetry [Fig. 1(c)]. The order of the uppermost valence states in CuCl is reversed, i.e., the Γ_7 states are higher in energy than the Γ_8 states since d states contribute to the spin-orbit splitting with opposite sign as compared to p orbitals.^{24,31,32} Due to the fact that the spin-orbit splitting of

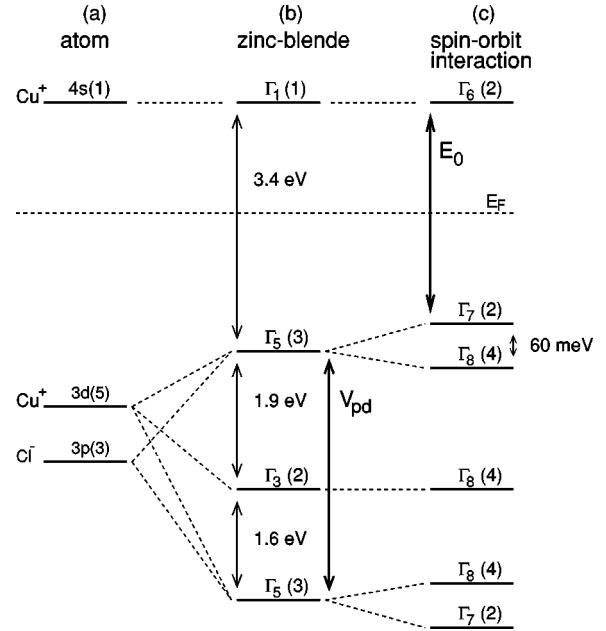


FIG. 1. Schematic derivation of the conduction and valence bands at the Γ point in CuCl (after Ref. 29). (a) Atomic levels of copper and chlorine, (b) partial lifting of the degeneracy of the d levels and hybridization in the cubic crystal field, and (c) spin-orbit splitting. The matrix element V_{pd} is responsible for the level splitting between hybridized p and d states (Ref. 11), which is indicated by the thick vertical arrow.

the atomic p orbitals increases with the atomic weight, the regular zinc-blende splitting scheme is recovered in the case of CuBr and CuI.

In the following we are interested in those $1s$ excitons only that derive from the Coulomb interaction between the electrons in the lowest conduction band $\Gamma_6(2)$ and the holes in the highest valence band $\Gamma_7(2)$. They are usually labeled Z_3 .²⁴ The short-range exchange interaction leads to a splitting of the Z_3 exciton into ortho- and paraexcitons having Γ_5 (threefold degenerate) and Γ_2 (nondegenerate) symmetry, respectively.³³ Optical transitions to orthoexcitons are one-photon allowed, while to first order the paraexciton is one-photon forbidden. The long-range exchange interaction splits the Γ_5 states into transverse and longitudinal orthoexcitons. The former exhibit a dispersion due to the formation of exciton polaritons when interacting with the light field. The exciton-polariton dispersions related to the Z_3 excitons are shown schematically in Fig. 2. LE1 labels the longitudinal exciton, Γ_2 the paraexciton, and TP1 and TP2 are the transverse orthoexciton-polariton branches. The light line is represented by the long-dashed line. A more detailed discussion can be found in Ref. 33.

Recent measurements have found a band gap of 3.3990(5) eV at 2 K and an effective Rydberg constant, \mathcal{R}^* of 130.6 ± 2.9 meV for the s series of the Z_3 exciton within a simple hydrogenlike model ($n \geq 2$).³⁴ The $1s$ exciton of Z_3 has a binding energy of 197 meV and therefore deviates strongly from the hydrogenlike model. The exciton binding energy depends on the appropriate dielectric constant ϵ and the reduced effective mass μ ($\mathcal{R}^* \sim \mu \epsilon^{-2}$). Both μ and ϵ depend on the size of the direct gap. As will be shown below, the temperature and isotope-mass dependence

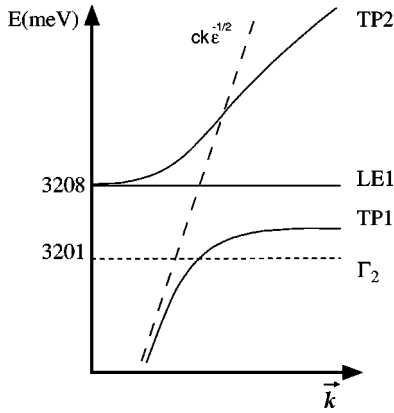


FIG. 2. Schematic sketch of the Z_3 exciton dispersion in CuCl.

of the CuCl band gap is small compared to its size. Hence we expect the temperature and isotope-mass dependence of the $Z_3(n=1)$ exciton binding energy to be very small. In fact, throughout the following analysis we assume \mathcal{R}^* to be constant and therefore identify the mass and temperature-dependent renormalization of the Z_3 exciton-polariton energies with the renormalization of the band gap itself.

III. EXPERIMENT

A. Samples

Natural copper and chlorine have two stable isotopes each (relative abundances: ^{63}Cu , 69.2%; ^{65}Cu , 30.8%; ^{35}Cl , 75.8%; and ^{37}Cl , 24.2%). The elements used to grow our samples were isotopically pure (99.9%) except for the enriched ^{37}Cl , which contained about 11% of ^{35}Cl , as determined by mass spectroscopy. In order to avoid trivial effects caused by varying chemical impurities and crystal quality we investigated samples from independent sources and confirmed that the Raman spectra for identical isotopic compositions coincide.⁹ The samples are usually platelets of up to 10 mm² surface area and a thickness of less than 0.1 mm. Using x-ray diffraction we determined the surfaces to have the [111] orientation. Most samples were grown by heating Cu metal with the desired isotopic composition in flowing HCl gas. For the samples made from isotopically pure HCl, purification of the initial reaction products was achieved by two successive sublimations under vacuum and a zone melting process. Then a transport method in a closed tube containing H₂ was used to grow platelets. Further details of the sample growth have been described elsewhere.³⁵

B. Optical spectroscopy

We have measured different components of the CuCl Z_3 exciton in the exciton-polariton regime. Nonlinear spectroscopy is established as a precise method to investigate these photon-exciton coupled states in wide-band-gap semiconductors.³³ Two-photon absorption (TPA) can be used to determine the energies of the lowest longitudinal 1s exciton (LE1) around 3208 meV (see Fig. 2) and the middle transverse polariton branch (TP2) around 3216.5 meV. LE1 is almost dispersionless and therefore best suited for the determination of isotope effects. In our case the TPA from LE1 was detected by monitoring the intensity of the “ ν_2 ” emis-

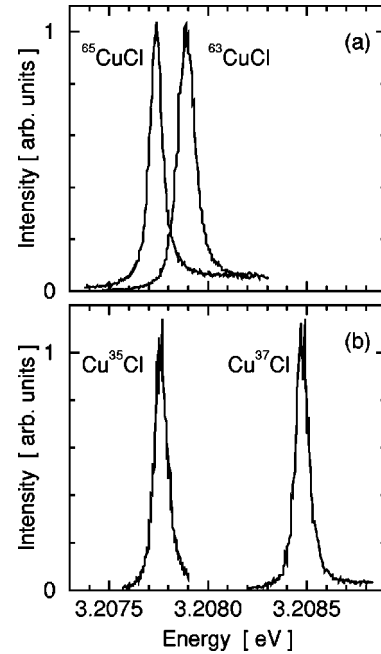


FIG. 3. Two-photon absorption in the region of the longitudinal exciton (LE1) in isotopically modified CuCl measured at 2 K.

sion line²¹ at 3179 meV as a function of two equienergetic photons, while their sum energy was scanned across the LE1 resonance.³⁶ The intensity of second-harmonic generation (SHG) was monitored in order to determine the TP2 energy close to $\vec{k}=\vec{0}$.³⁷ Luminescence spectra were excited using ~ 0.3 mW of the 3638-Å (3.408-eV) line of an Ar-ion laser. The scattered light was dispersed by a Spex 1404 double monochromator ($f=0.85$ m). Using single-photon counting, the spectra were recorded in backscattering geometry from a [111] surface. The spectra were calibrated against a nearby He-plasma line. In all measurements the samples were cooled to 1.8–2 K by immersion in superfluid helium and special care was taken to keep the sample heating at a minimum.

IV. RESULTS

We have investigated a batch of samples that covers a wide range of average copper and chlorine masses. We have measured nonlinear absorption spectra of the longitudinal exciton (LE1) and second-harmonic generation spectra of the transverse polariton (TP2) as well as the linear luminescence spectra of CuCl at low temperatures (2 K). For chlorine substitution we find the “regular” effect⁵ of an *increasing* gap when *increasing* the isotope masses of the compound. The TPA spectra of the LE1 excitons displayed in Fig. 3(b) show a shift of 357 $\mu\text{eV}/\text{amu}$ induced by the replacement of ^{35}Cl by ^{37}Cl in samples containing natural Cu. In contrast, LE1 *decreases* by 80 $\mu\text{eV}/\text{amu}$ when *increasing* the copper mass from ^{63}Cu to ^{65}Cu in samples that contain natural Cl [Fig. 3(a)]. In Fig. 4 we show results on TP2 obtained from the same samples using SHG. Again for *increasing* chlorine mass the gap *increases* by 323 $\mu\text{eV}/\text{amu}$ while it *decreases* by 86 $\mu\text{eV}/\text{amu}$ for *increasing* copper masses. In Fig. 5 we show the linear luminescence for natural CuCl and Cu³⁷Cl. A He-emission line (pl.) was used to calibrate the spectra.

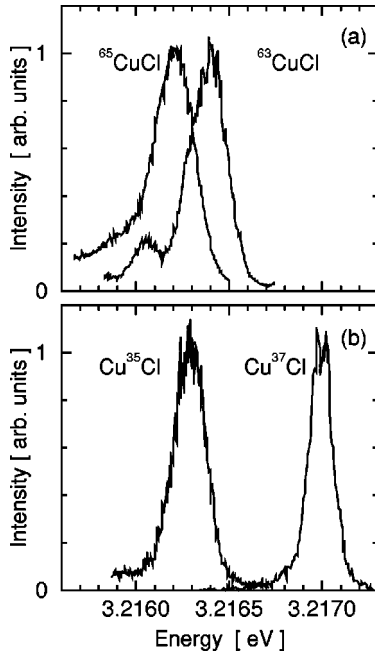


FIG. 4. Second-harmonic generation in the region of the transverse polariton (TP2) in isotopically modified CuCl measured at 2 K.

Three peaks can be identified as related to the TP2, TP1, and Γ_2 (ν_1 line in Ref. 21) excitons. Despite their considerable widths and/or ill-defined line shapes, we can extract average changes in the band gap, i.e., an *increase* of $400 \pm 50 \mu\text{eV}/\text{amu}$ for *increasing* chlorine mass. Note, however, that the shifts with Cu substitution are too small to be reliably measured with this technique. Nevertheless, they have been clearly observed using nonlinear spectroscopy.

We have summarized the energies of LE1 and TP2 obtained from CuCl samples of various isotopic compositions in Fig. 6, where the error bars represent an average of independent measurements on samples of nominally equivalent isotopic composition. The straight lines are linear fits to the data. Assuming that the mass dependence is the same for

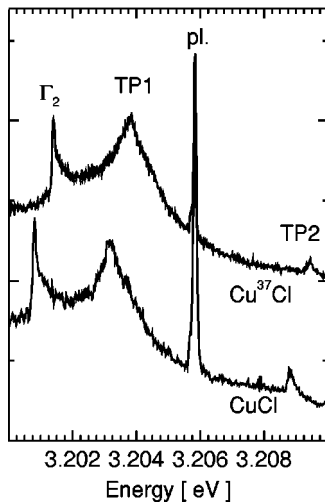


FIG. 5. Linear luminescence spectra of the Γ_2 paraexciton and transverse polaritons in CuCl at 2 K excited by the 3638 \AA (3.408 eV) Ar laser line; pl. denotes a He-plasma line.

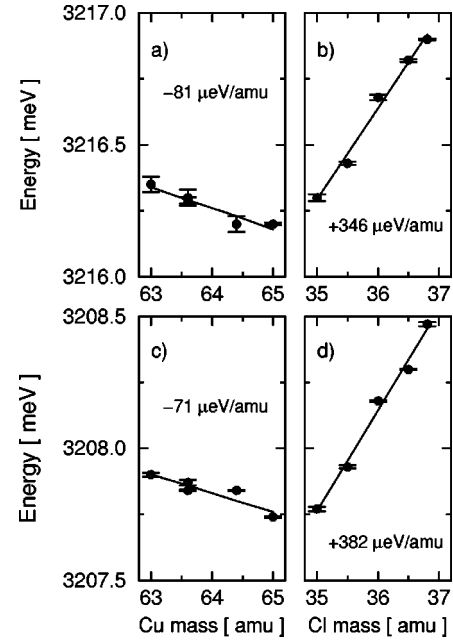


FIG. 6. Changes in the band gap of CuCl with isotopic composition measured for copper and chlorine substitution on (a) and (b) the transverse polariton TP2 and (c) and (d) the longitudinal exciton LE1.

LE1 and TP2+364(18), we obtain $\partial E_0/\partial M_{\text{Cu}} = -76(5) \mu\text{eV}/\text{amu}$ and $\partial E_0/\partial M_{\text{Cl}} = 364(18) \mu\text{eV}/\text{amu}$ for the change in the band gap with isotope substitution in CuCl at 2 K.

V. DISCUSSION

The mean-square amplitude of a phonon at one of the atoms participating in the vibration depends on its frequency, the atomic masses, its eigenvector, and the temperature. Isotope substitution as well as changes in the temperature result in slightly different vibrational amplitudes and phonon frequencies. This leads to changes in the band gap via the electron-phonon interaction.

A. Mass and temperature dependence of the fundamental gap

A method to calculate the temperature dependence of semiconductor band gaps based on local empirical pseudopotentials and lattice-dynamical models was developed in a series of articles³⁸ and subsequently extended to a calculation of the dependence on the isotope mass.^{5,12} Here we only summarize the main ideas and results. The dependence of the band gap on the isotopic composition at constant temperature comprises two contributions:^{5,12}

$$\left(\frac{\partial E_0}{\partial M_\kappa} \right)_T = \left(\frac{\partial E_0}{\partial M_\kappa} \right)_{\text{EP}} + \left(\frac{\partial E_0}{\partial M_\kappa} \right)_{\text{TE}}, \quad (1)$$

i.e., a contribution of the electron-phonon interaction (EP) at constant volume and a second term that arises from changes in the lattice constant. The latter takes anharmonic corrections to the crystal volume at low temperatures into account, which depend on the isotope masses through the zero-point vibrational amplitudes. It is labeled TE since its origin is analogous to that of the thermal expansion of the lattice.

The correction to the band gap arising from the dependence of the lattice constant on the isotope masses can be written as⁵

$$\left(\frac{\partial E_0}{\partial M_\kappa}\right)_{\text{TE}} = -3B \left(\frac{\partial E_0}{\partial p}\right)_M \left(\frac{\partial \ln a_0}{\partial M_\kappa}\right)_p, \quad (2)$$

where B is the bulk modulus, $(\partial E_0/\partial p)_M$ the change of the gap with pressure, and $(\partial \ln a_0/\partial M_\kappa)_p$ the relative change of the lattice constant a_0 when changing the mass of the atomic species κ . The pressure dependence of the CuCl LE1 energy at low temperatures, $(\partial \text{LE1}/\partial p)_M = 7.65(10)$ meV/GPa (see Ref. 39), is an order of magnitude smaller than in GaAs, ZnSe, or Ge.⁵ Furthermore, the bulk modulus of CuCl at room temperature [$B=45.9$ GPa (Refs. 14 and 15)] is smaller than in GaAs ($B=76$ GPa) and ZnSe ($B=65$ GPa).⁵ While the fractional change of the lattice constant with isotope substitution has not been directly measured for CuCl, we estimate from the temperature dependence of the lattice parameter⁴⁰ $(\partial \ln a_0/\partial M_{\text{Cl}})_p \approx -4 \times 10^{-5}$ 1/amu and $(\partial \ln a_0/\partial M_{\text{Cu}})_p \approx +5.4 \times 10^{-6}$ 1/amu. From these values we estimate a contribution of $\sim +40$ $\mu\text{eV}/\text{amu}$ for the substitution of ³⁵Cl by ³⁷Cl and ~ -6 $\mu\text{eV}/\text{amu}$ for that of ⁶³Cu by ⁶⁵Cu as compared with the measured values of $\partial E_0/\partial M_{\text{Cl}} = +364(18)$ $\mu\text{eV}/\text{amu}$ and $\partial E_0/\partial M_{\text{Cu}} = -76(5)$ $\mu\text{eV}/\text{amu}$. Although this is only a rough estimate of the isotope lattice expansion contribution, in view of its small value compared to the measured gap renormalization we feel justified in neglecting it. We note that in the case of GaAs and ZnSe the lattice expansion accounts for at most a third of the total gap renormalization.⁵

Hence we retain the renormalization of the band gap that stems from the electron-phonon interaction only. In principle, it can be calculated as follows:³⁸ The electron energy $E_n(\vec{k})$ of a band n is given by the unrenormalized energy $\epsilon_n(\vec{k})$ and a perturbation, i.e.,

$$E_n(\vec{k}) = \epsilon_n(\vec{k}) + \sum_{j,\vec{q}} \left(\frac{\partial E_n(\vec{k})}{\partial n_{j,\vec{q}}} \right) \left(n_{j,\vec{q}} + \frac{1}{2} \right). \quad (3)$$

The perturbation is the summation over coefficients $\partial E_n(\vec{k})/\partial n_{j,\vec{q}}$, which are weighted by the respective Bose-Einstein occupation number of the phonon (j,\vec{q}) . These coefficients are the sum of two contributions: a Debye-Waller term and the real part of the self-energy. The former term arises from the simultaneous interaction of an electron with two phonons from the branch j having the same wave vector \vec{q} (second-order electron-phonon interaction taken in first-order perturbation theory), while the latter term describes the electron-one-phonon interaction taken to second-order perturbation theory. The unrenormalized direct band gap is given by $E_0 = \epsilon_c(\vec{0}) - \epsilon_v(\vec{0})$. The total change of the gap as a function of the isotopic composition as well as its dependence on the temperature is thus the combination of the respective renormalizations of the valence and the conduction bands, i.e., $E_0(T,M) = E_c(\vec{0}) - E_v(\vec{0})$. In principle, the coefficients $\partial E_n(\vec{k})/\partial n_{j,\vec{q}}$ can be calculated, provided a good pseudopotential description of the electron bands and a good lattice-dynamical model are available.³⁸ While there is evidence⁹ that the 14-parameter shell model of Ref. 41 de-

scribes the phonon dispersion and eigenvectors of CuCl quite well, a satisfactory calculation of the CuCl band structure within a local-empirical pseudopotential framework is not available.¹¹ We note, however, that nonlocal empirical pseudopotential calculations of the CuCl band structure are available.²⁸ In the following we restrict ourselves to a simplified model.

B. Two-oscillator model

The phonon dispersion of CuCl exhibits a gap between the acoustic and the optic branches.⁴¹ Due to the relatively large mass difference between Cu and Cl, the acoustic-mode eigenvectors are dominated by copper displacements while those of the optic modes mostly involve chlorine displacements.⁹ Therefore, we approximate the lattice dynamics of CuCl, required for the gap renormalization, by two effective harmonic oscillators (Einstein models): One oscillator with an energy of $\omega_{\text{Cu}} = 1$ THz (33.3 cm^{-1}) represents an average acoustic, purely Cu-like phonon and a second oscillator with an energy of $\omega_{\text{Cl}} = 6$ THz represents an average optic, purely Cl-like phonon. This simplification is supported by the decomposition of the phonon density of states of CuCl in Ref. 41 obtained from neutron scattering experiments, where the averages for the Cu and Cl contributions are approximately at those frequencies. This approach has also been successfully applied to the gap shifts induced by temperature as well as by changes in the isotope masses in wurtzite CdS, a semiconductor in which both the electronic structure and the lattice dynamics are difficult to describe in simple terms.⁴² With this approximation the summation over all phonon states required to calculate the coefficients $\partial E_n(\vec{k})/\partial n_{j,\vec{q}}$ coalesces into two contributions. Lacking a detailed description of the electron bands n required to calculate $\partial E_n(\vec{k})/\partial n_{j,\vec{q}}$ (compare Ref. 5), we resort to approximating these coefficients by effective electron-phonon interaction parameters A_{Cu} and A_{Cl} . As a result we find for the total mass and temperature dependence of the fundamental gap

$$E_0(T,M) = E_0 + \frac{A_{\text{Cu}}}{\omega_{\text{Cu}} M_{\text{Cu}}} \left(n(\omega_{\text{Cu}}, T) + \frac{1}{2} \right) + \frac{A_{\text{Cl}}}{\omega_{\text{Cl}} M_{\text{Cl}}} \left(n(\omega_{\text{Cl}}, T) + \frac{1}{2} \right), \quad (4)$$

where E_0 , A_{Cu} , and A_{Cl} can be determined, e.g., from a fit to the experimentally determined temperature dependence of the gap. Taking into account the proportionality of $\omega_{\text{Cu/Cl}} \sim (M_{\text{Cu/Cl}})^{-1/2}$, we find the gap shifts due to the isotope substitution of either Cu or Cl at zero temperature to be

$$\frac{\partial E_0(T=0,M)}{\partial M_{\text{Cu/Cl}}} = -\frac{1}{4} \frac{A_{\text{Cu/Cl}}}{\omega_{\text{Cu/Cl}} M_{\text{Cu/Cl}}^2}. \quad (5)$$

In Fig. 7 we reproduce the experimental data for the temperature dependence of the Z_3 exciton energy in the range between $T=0$ and 350 K from Refs. 21–23. The fit of Eq. (4) to these data is shown as the solid line. We obtain an unrenormalized gap energy $E_0 = 3236$ meV, which is indicated by the solid horizontal line. It is instructive to examine

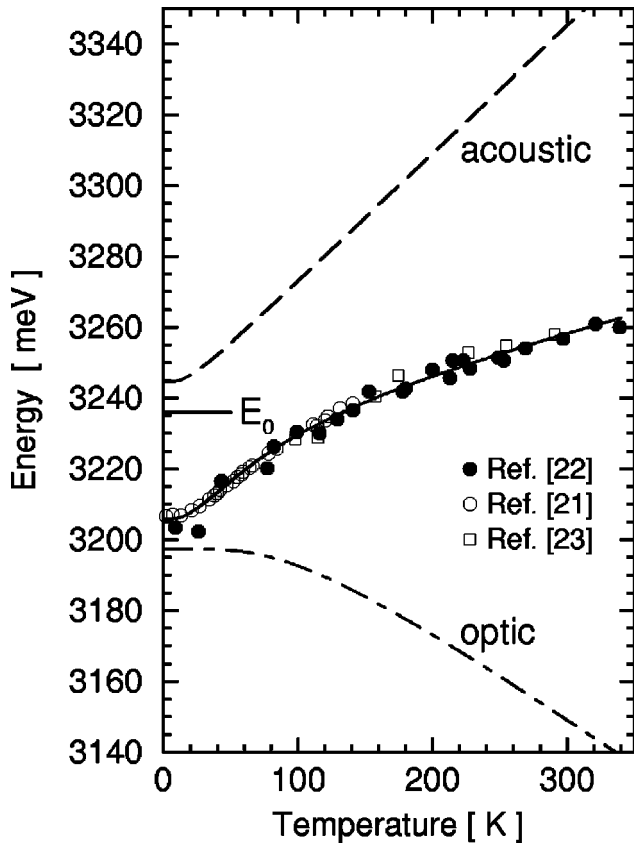


FIG. 7. Temperature dependence of the energy of the Z_3 exciton of CuCl. The solid line is the fit of a two-oscillator model, the dashed and the dash-dotted line show the individual contributions of the acoustic-frequency (Cu) and optic-frequency (Cl) oscillators.

the gap renormalization induced by the zero-point motion within the two-oscillator model: While the optic, chlorinlike vibration *reduces* the gap by 38.8 meV the acoustic, copperlike vibration *increases* the gap by 8.7 meV. Taking the temperature dependence into account we find that the low-frequency acoustic, copperlike vibrations are appreciably populated already at low temperatures and raise the band gap (dashed line in Fig. 7). For the high-frequency optic, chlorinlike vibrations we find that its negative contribution is almost constant up to about 70 K. Above 70 K the chlorinlike modes become substantially populated and their occupation results in an increasingly negative contribution. Taken together, this causes the band gap to increase strongly below 70 K (with increasing temperature) and to continue to increase, albeit with a significantly reduced slope, above 70 K. The kink in the temperature dependence is clearly visible in Fig. 7.

From the fit of Eq. (5) to the data in Fig. 7 we find $\partial E_0 / \partial M_{\text{Cu}} = -69(7) \mu\text{eV}/\text{amu}$ and $\partial E_0 / \partial M_{\text{Cl}} = +546(55) \mu\text{eV}/\text{amu}$ for the mass dependence of the fundamental gap at zero temperature.⁴³ This is in reasonable agreement with our experimental data of $-76(5) \mu\text{eV}/\text{amu}$ and $+364(18) \mu\text{eV}/\text{amu}$ for copper and chlorine substitution, respectively, and with the predictions of Ref. 11. Note that the coefficients determined by means of isotope substitution are much more precise than those inferred from the temperature dependence.

We can also explore a different approach: Taking the measured zero-temperature mass dependence of the band gap

(see Fig. 6) and fitting the measured temperature dependence (see Fig. 7) with Eq. (4) allows us to determine the frequencies of the two oscillators. We find values of $E_0 = 3221.2 \text{ meV}$, $\omega_{\text{Cu}} = 1.05 \text{ THz}$, and $\omega_{\text{Cl}} = 4.0 \text{ THz}$. Although the frequency of the chlorinlike oscillator is only two-thirds of our original assumption, overall we conclude that the two-oscillator model gives a consistent description of the distinctive changes in the CuCl band gap with isotope substitution and its exceptional temperature dependence.

Note that the importance of the copperlike vibrations for the anomalous gap shifts of CuCl can be understood in a local empirical pseudopotential approach.¹¹ When shifting remote d -like (copper) plane waves to a lower energy, so that they are close to the chlorine atomic p levels, and allowing for p - d mixing, it has been found that the resulting level splitting in the valence band (compare Fig. 1) is to a large extent determined by a Cu atomic pseudopotential. Introducing a Debye-Waller factor to “weaken” this pseudopotential with increasing temperature results in a decreasing hybridization energy. This lowers the top of the valence band and therefore the band gap increases with increasing temperature. For Cl substitution, however, the p - d mixing is almost unaffected. Along these lines gap shifts of $-85 \mu\text{eV}/\text{amu}$ for increasing Cu masses and $+970 \mu\text{eV}/\text{amu}$ for an increase in the chlorine mass have been predicted.¹¹ This is in qualitative agreement with the experiment.

C. Isotope effects in CuBr

As another application of the two-oscillator model we have taken the temperature dependence of the $Z_{1,2}$ and Z_3 excitons in CuBr from Ref. 44 and analyzed these data in the manner outlined above. While the structure of the valence band usually found in zinc-blende materials is also found in CuBr, i.e., the highest valence band is fourfold degenerate (Γ_8) and the spin-orbit split-off twofold degenerate band (Γ_7) is lower in energy, its band gap behaves unusually in that it increases with increasing temperature also. Using two oscillators with fixed frequencies $\omega_{\text{Cu}} = 1 \text{ THz}$ and $\omega_{\text{Br}} = 4.5 \text{ THz}$ for the acoustic, copperlike oscillators and the optic, brominlike oscillators, respectively,¹⁶ we have fitted Eq. (4) to the temperature dependences of the exciton energies. The results are shown in Fig. 8. From these fits and Eq. (5) we obtain $\partial E_0 / \partial M_{\text{Cu}} = -38(4) \mu\text{eV}/\text{amu}$ and $\partial E_0 / \partial M_{\text{Br}} = +78(8) \mu\text{eV}/\text{amu}$ for the mass dependence of the $Z_{1,2}$ exciton energy and $\partial E_0 / \partial M_{\text{Cu}} = -29(3) \mu\text{eV}/\text{amu}$ and $\partial E_0 / \partial M_{\text{Br}} = +45(5) \mu\text{eV}/\text{amu}$ for the mass dependence of the Z_3 exciton energy, where the errors reflect the variance corresponding to the fit. While the effect of Cu substitution is about the same as in CuCl, the gap change due to Br replacement is reduced by an order of magnitude as compared to CuCl. This is most likely due to the relatively small effect of changing the much larger Br mass by 1 amu. However, these values are only rough estimates since at low temperatures, i.e., in the important range that determines the copperlike oscillator, only a limited number of experimental data points are available. Furthermore, the distinction between an acoustic, copperlike and an optic, brominlike mode is questionable since copper and bromine have rather similar masses. Nevertheless, these fits support, at least qualitatively, the

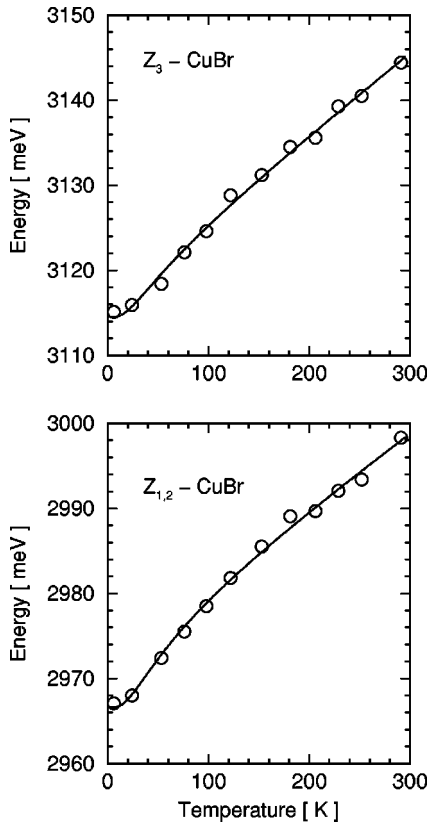


FIG. 8. Temperature dependence of the $Z_{1,2}$ and Z_3 excitons in CuBr. The solid lines are the fit of a two-oscillator model; data are from Ref. 44.

notion that p - d mixing has a strong influence on the electronic structure of CuBr and needs to be taken into account in its calculation.

VI. SUMMARY AND CONCLUSIONS

Isotope substitution is an excellent means to change the energies of vibrational excitations of a crystal. Therefore, it can be employed to study the band-gap renormalization that arises from the electron-phonon interaction in a well-defined manner. While it is clear that the magnitude of the band-gap renormalization decreases with increasing mass and, corre-

spondingly, increases with increasing temperature, the actual sign of the effect cannot be predicted easily. This sign arises from a delicate superposition of different contributions from the valence and conduction bands, which reflect the underlying lattice dynamics, the electronic structure, and the electron-phonon interaction.^{5,38} For diamond-structure and (most) zinc-blende semiconductors one finds a continuous net gap decrease with increasing temperature together with the corresponding mass effect $\partial E_0/\partial M_\kappa \geq 0$. CuCl and CuBr are very interesting materials since they provide an exception to this rule. Our study of the copper halides exposes the intricate, microscopic effects that contribute to the gap renormalization. The different contributions of acoustic and optic vibrations are revealed and, from the analysis of the isotope effect on the band gap, it becomes evident that its total renormalization encompasses a superposition of the individual contributions from the valence and conduction band. Studies of the electronic structure of the copper halides are complicated by the fact that their upper valence bands are mixed halide p states and copper d states. This is responsible for the unusual increase of the band gap with increasing temperature. Furthermore, these compounds exhibit an unusual negative mass coefficient ($\partial E_0/\partial M_{\text{Cu}} \leq 0$) when changing the copper mass, while the regular positive mass coefficient is recovered for halide substitution $\partial E_0/\partial M_X \geq 0$ for $X = \text{Cl}, \text{Br}$.

The effects of temperature and mass are related via the mean-square phonon amplitude. We have fitted the temperature dependence of the direct gap of CuCl and CuBr with a two-lattice-oscillator model and calculated the mass dependence of the band gap for the isotope substitution. These estimates are in very good agreement with our experimental data for CuCl, where we have found $\partial E_0/\partial M_{\text{Cu}} = -76(5) \mu\text{eV}/\text{amu}$ and $\partial E_0/\partial M_{\text{Cl}} = +364(18) \mu\text{eV}/\text{amu}$ for the respective isotope mass changes. We believe that our analysis provides a basis for crucial tests of first-principles calculations of the band structure and the electron-phonon interaction in the copper halides.

ACKNOWLEDGMENTS

We are indebted to V. Belitsky for his critical reading of the manuscript. J. W., M. S., and K. R. thank the Deutsche Forschungsgemeinschaft for financial support.

¹M. Cardona, in *Festkörperprobleme/Advances in Solid State Physics*, edited by R. Helbig (Vieweg, Braunschweig/Wiesbaden, 1994), Vol. 34, p. 35.

²A. K. Ramdas, *Solid State Commun.* **96**, 111 (1995).

³E. E. Haller, *J. Appl. Phys.* **77**, 2857 (1995).

⁴T. Ruf, H. D. Fuchs, and M. Cardona, *Phys. Bl.* **52**, 1115 (1996).

⁵N. Garro, A. Cantarero, M. Cardona, A. Göbel, T. Ruf, and K. Eberl, *Phys. Rev. B* **54**, 4732 (1996).

⁶A. Debernardi and M. Cardona, *Phys. Rev. B* **54**, 11 305 (1996).

⁷M. Asen-Palmer, K. Bartkowski, E. Gmelin, M. Cardona, A. P. Zhernov, A. V. Inyushkin, A. Taldenkov, V. I. Ozhogin, K. Itoh, and E. E. Haller, *Phys. Rev. B* **56**, 9431 (1997); W. S. Capinski, H. J. Maris, E. Bauser, I. Silier, M. Asen-Palmer, T. Ruf, M. Cardona, and E. Gmelin, *Appl. Phys. Lett.* **71**, 2109 (1997).

⁸D. T. Wang, A. Göbel, J. Zegenhagen, and M. Cardona, *Phys. Rev. B* **56**, 13 167 (1997); J. M. Zhang, M. Giehler, A. Göbel, T. Ruf, M. Cardona, E. E. Haller, and K. Itoh, *ibid.* **57**, 1348 (1998).

⁹A. Göbel, T. Ruf, M. Cardona, C. T. Lin, and J. C. Merle, *Phys. Rev. Lett.* **77**, 2591 (1996); A. Göbel, T. Ruf, C. T. Lin, M. Cardona, J. C. Merle, and M. Joucla, *Phys. Rev. B* **56**, 210 (1997).

¹⁰A. Göbel, D. T. Wang, M. Cardona, L. Pintschovius, W. Reichardt, J. Kulda, N. M. Pyka, K. Itoh, and E. E. Haller (unpublished).

¹¹N. Garro, A. Cantarero, M. Cardona, T. Ruf, A. Göbel, C. T. Lin, K. Reimann, S. Rübenaacke, and M. Steube, *Solid State Commun.* **98**, 27 (1996).

- ¹²S. Zollner, M. Cardona, and S. Gopalan, *Phys. Rev. B* **45**, 3376 (1992); C. Parks, A. K. Ramdas, S. Rodriguez, K. M. Itoh, and E. E. Haller, *ibid.* **49**, 14 244 (1994).
- ¹³T. Ruf, A. Göbel, M. Cardona, C. T. Lin, J. Wrzesinski, M. Steube, K. Reimann, N. Garro, A. Cantarero, J. C. Merle, and M. Joucla, in *The Physics of Semiconductors*, edited by M. Scheffler and R. Zimmermann (World Scientific, Singapore, 1996), p. 185.
- ¹⁴T. H. K. Barron, J. A. Birch, and G. K. White, *J. Phys. C* **10**, 1617 (1977).
- ¹⁵R. C. Hanson, K. Helliwell, and C. Schwab, *Phys. Rev. B* **9**, 2649 (1974).
- ¹⁶G. Kanellis, W. Kress, and H. Bilz, *Phys. Rev. Lett.* **56**, 938 (1986); *Phys. Rev. B* **33**, 8724 (1986); **33**, 8733 (1986).
- ¹⁷M. Krauzman, R. M. Pick, H. Poulet, G. Hamel, and B. Prevot, *Phys. Rev. Lett.* **33**, 528 (1974); M. L. Shand, H. D. Hochheimer, M. Krauzman, J. E. Potts, R. C. Hanson, and C. T. Walker, *Phys. Rev. B* **14**, 4637 (1976).
- ¹⁸Su-Huai Wei, S. B. Zhang, and Alex Zunger, *Phys. Rev. Lett.* **70**, 1639 (1993).
- ¹⁹C. H. Park and D. J. Chadi, *Phys. Rev. Lett.* **76**, 2314 (1996); **77**, 2592 (1996).
- ²⁰J. W. Kremer and K. H. Weyrich, *Phys. Rev. B* **40**, 9900 (1989); Cheng-Zhang Wang, R. Yu, and H. Krakauer, *Phys. Rev. Lett.* **72**, 368 (1994).
- ²¹F. Raga, R. Kleim, A. Mysyrowicz, J. B. Grun, and S. Nikitine, *J. Phys. (France) Colloq.* **28**, C3-116 (1967).
- ²²Y. Kaifu and T. Komatsu, *Phys. Status Solidi B* **48**, K125 (1971).
- ²³V. K. Miloslavskii and O. N. Yunakova, *Opt. Spectrosc.* **57**, 51 (1984).
- ²⁴M. Cardona, *Phys. Rev.* **129**, 69 (1963).
- ²⁵A. Zunger and M. L. Cohen, *Phys. Rev. B* **20**, 1189 (1979).
- ²⁶M. A. Khan, *Philos. Mag. B* **42**, 565 (1980).
- ²⁷H. Overhof, *Phys. Status Solidi B* **97**, 267 (1980).
- ²⁸M. Ferhat, A. Zaoui, C. Certier, and B. Khelifa, *Phys. Lett. A* **216**, 187 (1996); A. Zaoui, M. Ferhat, M. Certier, M. Soltani, and B. Khelifa, *Phys. Status Solidi B* **192**, 101 (1995).
- ²⁹A. Goldmann, *Phys. Status Solidi B* **81**, 9 (1977).
- ³⁰S. Lewonczuk, J. G. Gross, J. Ringeissen, M. A. Khan, and R. Riedinger, *Phys. Rev. B* **27**, 1259 (1983).
- ³¹S.-H. Wei and A. Zunger, *Phys. Rev. B* **37**, 8958 (1988); D. Vogel, P. Krüger, and J. Pollmann, *ibid.* **52**, R14 316 (1995).
- ³²K. Shindo, A. Morita, and H. Kamimura, *J. Phys. Soc. Jpn.* **20**, 2054 (1965).
- ³³D. Fröhlich, P. Köhler, W. Nieswand, and E. Mohler, *Phys. Status Solidi B* **167**, 147 (1991); D. Fröhlich, in *Nonlinear Spectroscopy of Solids: Advances and Applications*, edited by B. Di Bartolo and B. Bowlby (Plenum Press, New York, 1994), p. 289; B. Hönerlage, R. Lévy, J. B. Grun, C. Klingshirn, and K. Bohnert, *Phys. Rep.* **124**, 161 (1985).
- ³⁴K. Saito, M. Hasuo, T. Hatano, and N. Nagasawa, *Solid State Commun.* **94**, 33 (1995).
- ³⁵C. T. Lin, E. Schönherr, A. Schmeding, T. Ruf, A. Göbel, and M. Cardona, *J. Cryst. Growth* **167**, 612 (1996).
- ³⁶D. Fröhlich, E. Mohler, and P. Wiesner, *Phys. Rev. Lett.* **26**, 554 (1971).
- ³⁷D. C. Haueisen and H. Mahr, *Phys. Rev. Lett.* **26**, 838 (1971).
- ³⁸P. B. Allen and M. Cardona, *Phys. Rev. B* **27**, 4760 (1983); P. Lautenschlager, P. B. Allen, and M. Cardona, *ibid.* **31**, 2163 (1985); S. Gopalan, P. Lautenschlager, and M. Cardona, *ibid.* **35**, 5577 (1987); P. B. Allen, *Philos. Mag. B* **70**, 527 (1994).
- ³⁹K. Reimann and St. Rübenacke, *Phys. Rev. B* **49**, 11 021 (1994).
- ⁴⁰*Physics of Group II-VI and I-VII Compounds*, edited by O. Madelung, M. Schulz, and H. Weiss, Landolt-Börnstein, New Series, Group III, Vol. 17, Pt. b (Springer, Berlin, 1982).
- ⁴¹B. Hennion, B. Prevot, M. Krauzman, R. M. Pick, and B. Dorner, *J. Phys. C* **12**, 1609 (1979); B. Prevot, B. Hennion, and B. Dorner, *ibid.* **10**, 3999 (1977).
- ⁴²J. M. Zhang, T. Ruf, R. Lauck, and M. Cardona, *Phys. Rev. B* **57**, 9716 (1998).
- ⁴³Due to a numerical error, the values for these gap shifts given in Ref. 13 are a factor of 2 too large.
- ⁴⁴S. Lewonczuk, J. G. Gross, and J. Ringeissen, *J. Phys. (France) Lett.* **42**, L91 (1981).